JACS
JOURNAL OF THE AMERICAN CHEMICAL SOCIETY

ARTICLE

pubs.acs.org/JACS

Quadrupole Central Transition ^{17}O NMR Spectroscopy of Biological Macromolecules in Aqueous Solution

Jianfeng Zhu and Gang Wu*

Department of Chemistry, Queen's University, 90 Bader Lane, Kingston, Ontario, Canada K7L 3N6

Supporting Information

ABSTRACT: We demonstrate a general nuclear magnetic resonance (NMR) spectroscopic approach in obtaining high-resolution ^{17}O (spin-5/2) NMR spectra for biological macromolecules in aqueous solution. This approach, termed quadrupole central transition (QCT) NMR, is based on the multiexponential relaxation properties of half-integer quadrupolar nuclei in molecules undergoing slow isotropic tumbling motion. Under such a circumstance, Redfield's relaxation theory predicts that the central transition, $m_I = +1/2 \leftrightarrow -1/2$, can exhibit relatively long transverse relaxation time constants, thus giving rise to relatively narrow spectral lines. Using three robust protein−ligand complexes of size ranging from 65 to 240 kDa, we have obtained ^{17}O QCT NMR spectra with unprecedented resolution, allowing the chemical environment around the targeted oxygen atoms to be directly probed for the first time. The new QCT approach increases the size limit of molecular systems previously attainable by solution ^{17}O NMR by nearly 3 orders of magnitude (1000-fold). We have also shown that, when both quadrupole and shielding anisotropy interactions are operative, ^{17}O QCT NMR spectra display an analogous transverse relaxation optimized spectroscopy type behavior in that the condition for optimal resolution depends on the applied magnetic field. We conclude that, with the currently available moderate and ultrahigh magnetic fields (14 T and higher), this ^{17}O QCT NMR approach is applicable to a wide variety of biological macromolecules. The new ^{17}O NMR parameters so obtained for biological molecules are complementary to those obtained from ^{1}H, ^{13}C, and ^{15}N NMR studies.

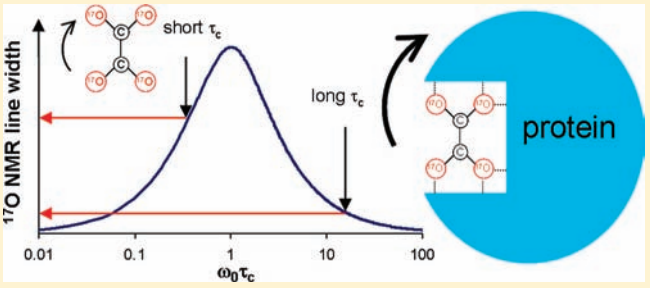

1. INTRODUCTION

Nuclear magnetic resonance (NMR) spectroscopy is a powerful analytical technique that can yield detailed information about chemical bonding, molecular structure, and dynamics. For biological macromolecules such as proteins and nucleic acids, most successful NMR applications to date have relied primarily on detection of spin-1/2 nuclei (i.e., ^{1}H, ^{13}C, ^{15}N, and ^{31}P). Among the most abundant elements found in biological macromolecules, oxygen remains the only one that has not been readily accessible by NMR spectroscopy. This is primarily because the only NMR-active, stable oxygen isotope, ^{17}O, has a quadrupolar nucleus (I = 5/2). It is well-known that quadrupolar nuclei often give rise to NMR spectra with very poor spectral resolution. As a result, NMR studies of quadrupolar nuclei are far less common than those of spin-1/2 nuclei. For the same reason, ^{17}O NMR applications have rarely gone beyond the realm of small organic and inorganic molecules over the past several decades.[1−6] One commonly accepted argument against attempting ^{17}O NMR experiments for biological macromolecules in solution is that, for a slowly tumbling macromolecule, the ^{17}O quadrupole relaxation would be so rapid that the ^{17}O NMR signals become too broad to be detectable, even when the level of ^{17}O (natural abundance 0.037%) can be enriched to 100%. Hence, solid-state ^{17}O NMR has been considered to be the only alternative that may permit the detection of ^{17}O NMR signals in large molecular systems.[7−9] Indeed, several research groups have recently made important advances in the development of solid-state ^{17}O NMR spectroscopy for studying biological systems.[10−22]

In the wake of these recent successes in solid-state ^{17}O NMR studies of organic and biological molecules, we had also come to question the conventional wisdom about the *infeasibility* of ^{17}O NMR in studying large molecular systems in aqueous solution. It turned out that the aforementioned common argument against solution ^{17}O NMR applications to macromolecular systems is entirely false. That argument is based on a simple extrapolation from equations that are only valid when the molecular motion satisfies the so-called extreme narrowing condition (i.e., $\omega_0\tau_c \ll 1$, where ω_0 is the Larmor angular frequency of the nucleus under detection and τ_c is the molecular rotational correlation time). However, with modern superconducting magnets, the tumbling motion of a biological macromolecule in aqueous solution is nearly always in the slow motion limit from the ^{17}O NMR point of view (i.e., $\omega_0\tau_c \gg 1$), rather than in the extreme narrowing limit. The quadrupole relaxation properties in these two motion regions can be completely different. In fact, the nuclear spin relaxation theory for quadrupolar nuclei has been established for many decades.[23−33] This relaxation theory suggests that the

Received: September 2, 2010
Published: December 22, 2010

dx.doi.org/10.1021/ja1079207 | *J. Am. Chem. Soc.* 2011, 133, 920–932

transverse relaxation process of a half-integer quadrupole nucleus is multiexponential, and as such, the resultant NMR spectrum should consist of $I + 1/2$ superimposed Lorentzian lines. Most importantly, among these $I + 1/2$ exponential components, the one associated with the central transition (CT), $m_I = +1/2 \leftrightarrow -1/2$, can have relatively long transverse relaxation times in the slow motion limit. Therefore, it is entirely possible to obtain narrow lines in NMR spectra of half-integer quadrupolar nuclei in solution, as long as the molecular tumbling is in the slow motion limit. The particular NMR method that focuses on detection of the CT signals was termed quadrupole central transition (QCT) spectroscopy by previous workers.[34,35] However, this multiexponential relaxation behavior of half-integer quadrupolar nuclei, although known for many years, has not been widely appreciated. Over the past several decades, only on a few occasions have researchers utilized it, primarily in studies of metal ions such as ^{51}V (spin-7/2),[34,36] ^{27}Al (spin-5/2),[37−40] ^{43}Ca (spin-7/2),[41,42] ^{45}Sc (spin-7/2),[43] and $^{69/71}$Ga (spin-3/2)[44] in metalloproteins and in studies of multiple-quantum NMR for quadrupolar nuclei.[45−47] Despite these pioneering studies, the common misconception about NMR of quadrupolar nuclei in liquids appears to have remained largely unchanged to date. We should also note two other areas in which multiexponential quadrupole relaxation has been shown to be important. One is related to the interference effects between quadrupolar and dipolar interactions which can be observed in the spectra of spin-1/2 nuclei when they are *J*-coupled to quadrupolar nuclei.[48−51] The other is concerned with various dynamic processes in solid materials.[52−54]

While most solution ^{17}O NMR studies in the literature discussed quadrupole relaxation processes only in the context of the extreme narrowing condition, there were indeed two occasions where researchers recognized the distinct multiexponential relaxation properties of ^{17}O in the slow motion limit. In particular, Gerlt and colleagues[55] pointed out that it is possible to have relatively long ^{17}O transverse relaxation times when $\omega_0\tau_c \gg 1$. Oldfield and colleagues[56,57] reported the first ^{17}O NMR spectra for C^{17}O ligands bound to proteins (peroxidases, myoglobins, and hemoglobins) in aqueous solution. They found that, in these cases, the values of $\omega_0\tau_c$ are ranged between 5.8 and 10 and that the observed ^{17}O NMR signals for protein-bound C^{17}O ligands exhibit relatively narrow line widths (ca. 200 Hz at 11.7 T). However, because the ^{17}O nuclear quadrupole coupling constant (C_Q) in C^{17}O is known to be notoriously small (C_Q < 1 MHz), it is not entirely clear whether the multiexponential relaxation properties of ^{17}O can be utilized as a general method for studying other oxygen-containing functional groups where much larger C_Q values are usually expected (ca. C_Q = 6−20 MHz). Perhaps because of this kind of doubt, there had been no follow-up solution ^{17}O NMR applications to biological macromolecules for more than 20 years since the pioneering work of Oldfield and colleagues.[56,57] Recently, we have reported some preliminary ^{17}O QCT NMR results for large protein−ligand complexes in aqueous solution and concluded that ^{17}O QCT is applicable to almost all oxygen-containing functional groups.[58] In the present work, we report a comprehensive evaluation of the ^{17}O QCT approach for studying biological macromolecules in aqueous solution. The primary objective of this work is to further demonstrate the general applicability of ^{17}O QCT spectroscopy. Here we will present a unified theoretical treatment of the quadrupole relaxation processes for spin-5/2 nuclei over several different regimes of molecular motion, outline the basic principles of QCT spectroscopy, and report new experimental ^{17}O QCT NMR results on three robust protein−ligand complexes of size ranging from 65 to 240 kDa.

2. EXPERIMENTAL SECTION

Ovotransferrin (OTf) from chicken egg white (EC 215.727.0) (BioUltra grade, lot no. 107K7022, agarose electrophoresis purity 99%), pyruvate kinase (PK) from rabbit muscle (EC 2.7.1.40) (lot no. 047K1512, protein purity 57%), avidin from egg white (EC 215.783.6) (lot no. 026K7044, SDS−PAGE purity 98%), and (+)-biotin 4-nitrophenyl ester (99%, purity) were purchased from Sigma-Aldrich (Oakville, Ontario, Canada). Oxalic acid (1,2-$^{13}C_2$, 99%) was purchased from Cambridge Isotope Laboratories, Inc. (CIL, Andover, Massachusetts). Sodium [$^{17}O_4$]oxalate was prepared by first dissolving 50 mg of oxalic acid in 0.3 mL of ^{17}O-enriched H_2O (70% ^{17}O atom), heating the solution at 50−55 °C overnight, and then neutralizing the solution with dry NaOH. The ^{17}O-enriched water was recovered on a vacuum line. [$^{17}O_2$]Biotin was prepared by base-catalyzed hydrolysis of (+)-biotin 4-nitrophenyl ester in CH_3OH/CH_2Cl_2 using Na^{17}OH (45% ^{17}O atom).

The OTf−Al−[$^{17}O_4$]oxalate complex was prepared in the following fashion. Approximately 80 mg of OTf was dissolved in 0.75 mL of H_2O, followed by addition of $Al(NO_3)_3$ and $Na_2C_2[^{17}O_4]$ to reach a molar ratio of approximately Al:oxalate:OTf = 2:2:1. The protein concentration was determined by the absorption at 280 nm on an HP 8452A diode array UV−vis spectrophotometer using a molar extinction coefficient (ε) of 91 200 M^{-1} cm^{-1}. KCl was also added to the protein solution to a final concentration of 150 mM. The final pH of the solution was adjusted to 7.5 using NaOH. The amount of free [$^{17}O_4$]oxalate ligands in the protein sample was monitored by solution ^{17}O NMR. Excess [$^{17}O_4$]oxalate ligands were removed by ultrafiltration (5−6 times) using Millipore Amicon Ultra filter units with a molecular mass cutoff of 3000 Da (Fisher Scientific, Ottawa, Canada). The PK−Mg(II)−[$^{17}O_4$]oxalate complex was prepared in tris(hydroxymethyl)aminomethane (TRIS or THAM) buffer solution (pH 7.5). Approximately 80 mg of PK was dissolved in 0.2 mL of TRIS buffer solution, followed by addition of $MgCl_2$, Na_2(5′-ATP), and $Na_2C_2[^{17}O_4]$, to reach a molar ratio of approximately Mg:ATP:oxalate:PK = 16:8:4:1 (theoretical 8:4:4:1). The protein concentration was determined by the absorption at 280 nm (ε = 128 520 M^{-1} cm^{-1}). Excessive amounts of Mg^{2+} and ATP were added to ensure that proteins were saturated with oxalate ligands. NaCl was also added to the protein solution to a final concentration of 75 mM. In some cases, more PK was added to minimize the concentration of free [$^{17}O_4$]oxalate ligands. The avidin−[$^{17}O_2$]biotin complex was prepared in the phosphate buffer (pH 7.4) with a small excessive amount of biotin as monitored by ^{17}O NMR.

Solution ^{17}O NMR experiments were performed using Bruker Avance-500 (11.74 T), Avance-600 (14.09 T), and Avance-II 900 (21.14 T) NMR spectrometers operating at 67.8, 81.3, and 122.0 MHz for ^{17}O nuclei, respectively. Typically, 80−100 μL of solution was transferred into either a 4 mm MAS rotor or a glass tube (4 mm o.d.). Bruker MAS probes were used at all three magnetic fields. A liquid sample of H_2O was used for radio frequency (RF) field strength calibration as well as for ^{17}O chemical shift referencing (δ = 0 ppm). For ^{17}O QCT NMR experiments, the effective 90° pulse is approximately one-third of that calibrated using a liquid H_2O sample. The ^{17}O spin−lattice relaxation times were measured using the saturation recovery method. Other detailed acquisition parameters are given in the appropriate figure captions.

3. THEORY

3.1. Quadrupole Relaxation Processes. Although the general theory of nuclear spin relaxation for half-integer quadrupolar nuclei has been well established for many decades,[23−33] its applications have been far less common in the literature than those for spin-1/2 nuclei. As a result, the distinct features of quadrupole relaxation properties are not widely known. Furthermore, oversimplified theoretical models used in most NMR textbooks with respect to quadrupole relaxation processes have

led to the well-spread misconception that high resolution cannot be obtained in NMR spectra of quadrupolar nuclei in the context of biological macromolecules in aqueous solution. Using results available in the literature, we present herein a theoretical background on the relaxation properties of spin-5/2 nuclei in isotropic liquids. The objective of this section is to give a unified treatment of nuclear quadrupole relaxation processes in the framework of Redfield's relaxation theory *over three distinct regimes of molecular motion*.

For a nuclear spin system containing spin-5/2 nuclei, the nuclear electric quadrupole interaction is described by a second-rank tensor known as the quadrupole coupling (QC) tensor whose three principal components are defined as χ_{ii} ($ii = xx, yy,$ and zz). These principal tensor components are related to those of the electric field gradient (EFG) tensor, eq_{ii}, in the following manner:

$$\chi_{ii}\,(\mathrm{MHz}) = e^2Qq_{ii}/h \tag{1}$$

where Q is the nuclear quadrupole moment of the nucleus under study, e is the elementary charge, and h is Planck's constant. The three principal components of an EFG tensor are not independent, because they must satisfy the condition $eq_{zz} + eq_{yy} + eq_{xx} = 0$. Thus, we also have $\chi_{zz} + \chi_{yy} + \chi_{xx} = 0$. In this study, we use the convention introduced by Cohen and Reif[59] for naming the EFG tensor components: $|eq_{zz}| \geq |eq_{yy}| \geq |eq_{xx}|$ or equivalently $|\chi_{zz}| \geq |\chi_{yy}| \geq |\chi_{xx}|$. In general, the two quantities that can be directly determined from NMR spectral analyses are known as the nuclear quadrupole coupling constant (C_Q) and the asymmetry parameter (η_Q):

$$C_Q = \chi_{zz} = e^2Qq_{zz}/h \tag{2}$$

$$\eta_Q = (\chi_{xx} - \chi_{yy})/\chi_{zz} = (eq_{xx} - eq_{yy})/eq_{zz} \quad (0 \leq \eta_Q \leq 1) \tag{3}$$

Since very often C_Q and η_Q are coupled together, especially in the context of quadrupole relaxation studies, it is more convenient to define another parameter, P_Q, known as the quadrupole product parameter, in the following fashion:

$$P_Q = C_Q\sqrt{1 + \frac{{\eta_Q}^2}{3}} \tag{4}$$

For spin-5/2 nuclei in a strong magnetic field, the nuclear Zeeman energy levels are shown in Figure 1. In NMR experiments of liquid samples where molecules undergo isotropic tumbling, the quadrupole interaction is often the predominant relaxation mechanism. Under such a circumstance, the time evolutions of the density matrix elements, σ_{ij}, that are associated with single-quantum coherences (related to the transverse magnetization) and populations (related to the longitudinal magnetization) are determined by the two sets of differential equations. Details about these differential equations and the corresponding transverse and longitudinal Redfield relaxation matrices for spin-5/2 nuclei are given in the Supporting Information. In general, the time evolution of the total transverse magnetization for spin-5/2 nuclei contains three distinct exponential components. Not only could these three components have different decaying rates, they could also exhibit different resonance frequencies as a result of the so-called dynamic frequency

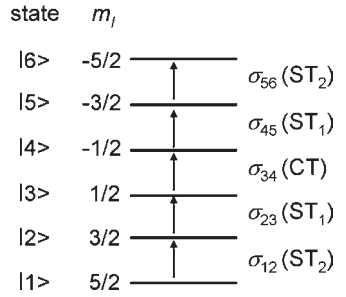

Figure 1. Zeeman energy levels, state labels, and density matrix elements corresponding to single-quantum coherences for $I = 5/2$ nuclei. CT = central transition, ST_1 = first satellite transition, and ST_2 = second satellite transition.

shifts. Therefore, a complete description of the time evolution of the total transverse magnetization for spin-5/2 nuclei should be written as

$$M_{x,y}(t) = \sum_{n=\mathrm{I,II,III}} A_n^{(2)} \exp[-(\mathrm{i}\Omega_n + R_n^{(2)})t] \tag{5}$$

where $A_n^{(2)}$, Ω_n, and $R_n^{(2)}$ are the amplitude, dynamic (angular) frequency shift, and transverse relaxation rate for the nth component, respectively. Components I, II, and III are related to the CT, first satellite transition (ST_1), and second satellite transition (ST_2) as defined in Figure 1. The analytical expressions for dynamic (angular) frequency shifts have been given previously by Werbelow:[30]

$$\Omega_{\mathrm{I}} = \frac{3\pi^2}{1000}{P_Q}^2(-16Q_1 + 16Q_2) \tag{6}$$

$$\Omega_{\mathrm{II}} = \frac{3\pi^2}{1000}{P_Q}^2(-4Q_1 + 10Q_2) \tag{7}$$

$$\Omega_{\mathrm{III}} = \frac{3\pi^2}{1000}{P_Q}^2(32Q_1 - 8Q_2) \tag{8}$$

Q_n ($n = 1, 2$) corresponds to the imaginary part of the normalized spectral density function and is related to the real part of the function, J_n ($n = 0, 1, 2$), in the following way:

$$Q_n = n\omega_0\tau_c J_n \tag{9}$$

$$J_n = \frac{\tau_c}{1 + (n\omega_0\tau_c)^2} \tag{10}$$

Similarly, the recovery of the longitudinal magnetization also has three exponential components:

$$M_z(t) - M_z(t = \infty) = \sum_{n=\mathrm{I,II,III}} A_n^{(1)} \exp(-R_n^{(1)}t) \tag{11}$$

where $A_n^{(1)}$ and $R_n^{(1)}$ are the amplitude and longitudinal relaxation rate for the nth component, respectively.

For spin-5/2 nuclei, one cannot obtain general analytical expressions for the amplitudes (A_{I}, A_{II}, and A_{III}) and the relaxation rates ($R^{(2)}$ and $R^{(1)}$) given in eqs 5 and 11. However, these quantities can be easily obtained through numerical calculations.

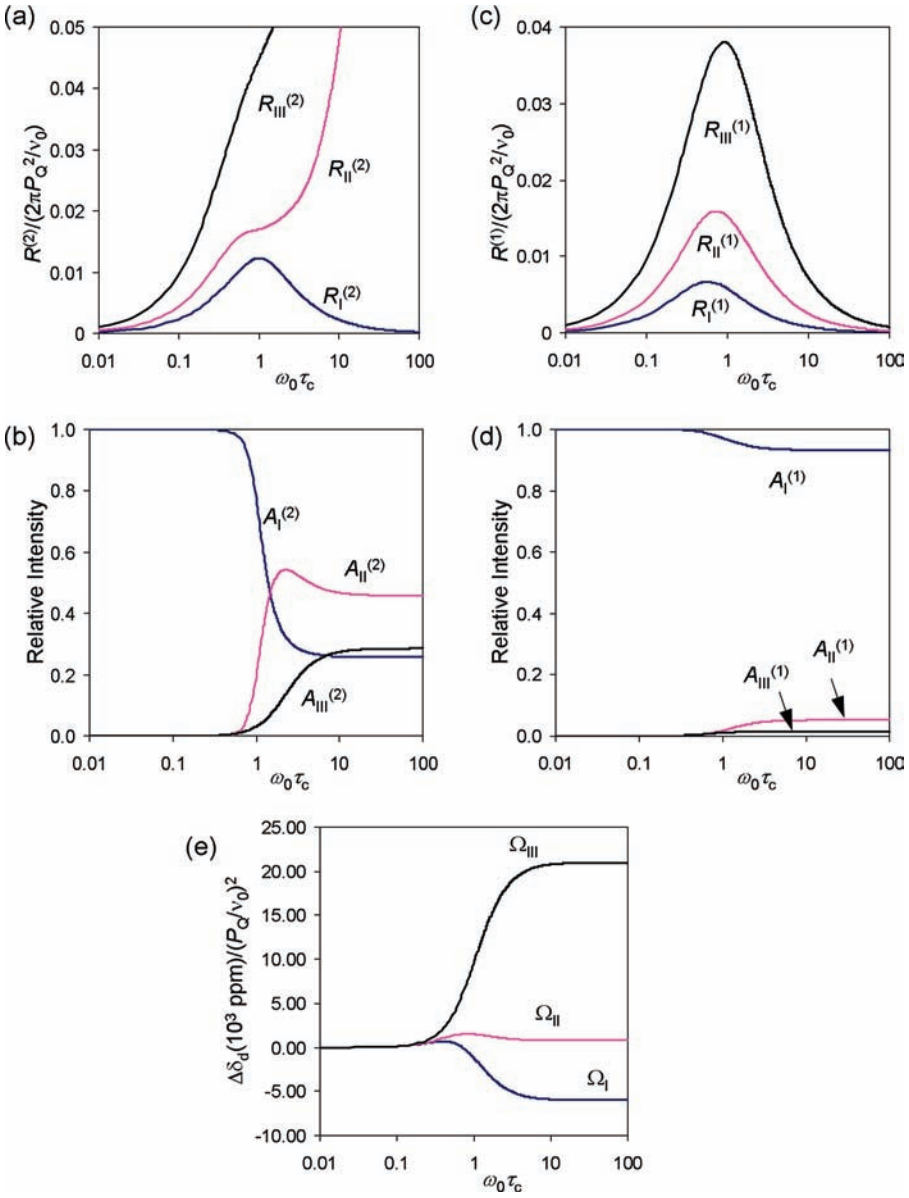

Figure 2. Theoretical results for (a) transverse relaxation rates and (b) corresponding amplitudes, (c) longitudinal relaxations rates and (d) corresponding amplitudes, and (e) dynamic frequency shifts (ppm) for spin-5/2 nuclei. See the text for a discussion.

Figure 2 shows the complete results for these quantities from numerical calculations for spin-5/2 nuclei. We should point out that identical results have been reported previously by Bull et al.[28] and by Chung and Wimperis.[47] Figure 2 also displays the dynamic frequency shifts as a function of $\omega_0\tau_c$ for spin-5/2 nuclei. Here it is often more convenient to define the dynamic frequency shift in parts per milion to be consistent with the chemical shift scale:

$$\Delta\delta_d = \frac{\Omega}{2\pi\nu_0} \times 10^6 \qquad (12)$$

where ν_0 is the Larmor frequency of the nucleus under detection, $\nu_0 = \omega_0/2\pi$. The results shown in Figure 2e are identical to those first derived by Werbelow[29] and by Werbelow and Pouzard.[30] It can be seen that $\Delta\delta_d$ for the CT (component I) is nearly always negative whereas $\Delta\delta_d$ for the ST_1 (component II) is essentially negligible. It should also be noted that, although $\Delta\delta_d$ for the ST_2 (component III) is much larger than those for the other two components, it can never be observed in practice, either because of its negligible amplitude or because of its excessive line width (vide infra).

Using the numerical results shown in Figure 2, we can calculate theoretical NMR spectra for spin-5/2 nuclei over a large range of molecular motion (i.e., from $\omega_0\tau_c \ll 1$ to $\omega_0\tau_c \gg 1$). To illustrate some of the important spectral features, we present in Figure 3 a series of theoretical ^{17}O NMR spectra using typical ^{17}O NMR parameters. When $\omega_0\tau_c \leq 0.5$, each spectrum exhibits a single Lorentzian line with the line width being proportional to τ_c. When $\omega_0\tau_c$ is between 1 and 5, the multi-Lorentzian features start to appear. However, although each spectrum should, in principle, be tri-Lorentzian, the third component is either too weak or too broad to be visible. As a result, each spectrum is practically always bi-Lorentzian in this motional range. When

dx.doi.org/10.1021/ja1079207 |J. Am. Chem. Soc. 2011, 133, 920–932

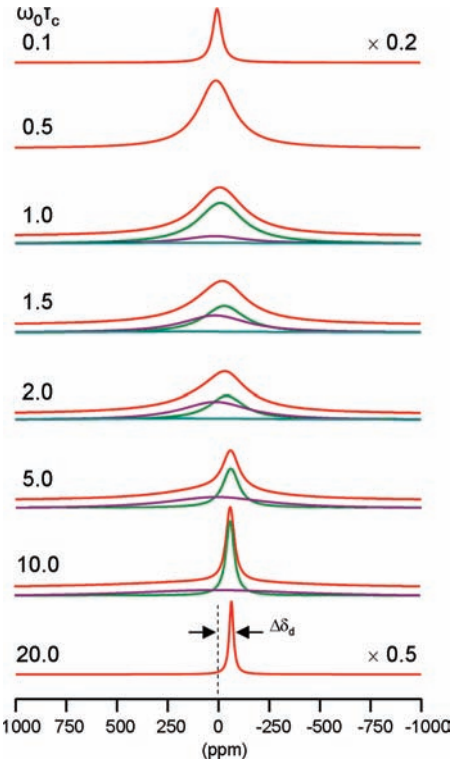

Figure 3. Theoretical ^{17}O NMR line shapes as a function of $\omega_0\tau_c$. All spectra were calculated using the numerical results shown in Figure 2 and the following parameters: P_Q = 8.5 MHz, δ_{iso} = 0 ppm, and ν_0 = 81.36 MHz (14.09 T). The total line shapes are shown in red, and individual components are shown in green, blue, and purple.

$\omega_0\tau_c$ exceeds 5, only the CT can be detected and the spectrum shows a single Lorentzian line once again. Most importantly, in this slow motion limit, the Lorentzian line from the CT can even be narrower than those observed under the extreme narrowing condition. In addition, the dynamic frequency shift causes the CT signal to appear at a lower frequency position from the true chemical shift position, as indicated in Figure 3.

In the discussion that follows, we will further examine the quadrupole relaxation properties for spin-5/2 nuclei in three different motion regimes: (1) fast ($\omega_0\tau_c \ll 1$), (2) intermediate ($\omega_0\tau_c \approx 1$), and (3) slow ($\omega_0\tau_c \gg 1$). The benefit of separating motion into these categories is that it is now possible to obtain analytical expressions from which one may gain deeper insight.

3.1.1. Fast Motion Limit. For small organic molecules in moderate magnetic fields, it is usually true that $\omega_0\tau_c \ll 1$. As mentioned earlier, this condition is also known as the extreme narrowing condition. Under such a circumstance, all spectral density functions have the same value, i.e., $J_0 = J_1 = J_2 = \tau_c$. Consequently, the transverse and longitudinal quadrupole relaxation processes have the same rate:

$$R^{(2)} = R^{(1)} = R_I^{(2)} = R_I^{(1)} = \frac{12\pi^2}{125} P_Q{}^2 \tau_c \qquad (13)$$

It is clear that eq 13 predicts that the line width of the NMR signal from a quadrupolar nucleus increases with τ_c. This equation is often introduced in most NMR textbooks when quadrupole relaxation processes are discussed. However, it is important to emphasize that this equation is only valid under the extreme narrowing condition. As noted earlier, a common mistake is to apply eq 13 to systems that are in the slow motion regime. Ironically, as will be shown in the next section, the line width of the NMR signal from systems that are in the slow motion regime exhibits a trend exactly opposite that described by eq 13.

3.1.2. Intermediate Motion Region. If $\omega_0\tau_c \approx 1$, $J_0 \geq J_1 \geq J_2$; this situation is often referred to as the intermediate motion region or the near extreme narrowing condition. In principle, both the transverse and longitudinal processes contain three exponential components. However, Halle and Wennerström[60] showed that, in this motion regime, both transverse and longitudinal relaxation processes can be approximated to be "nearly exponential". Using a perturbation treatment, these workers obtained the following analytical expressions for quadrupole relaxation rates:[60]

$$R^{(2)} = \frac{6\pi^2}{625} P_Q{}^2 (3J_0 + 5J_1 + 2J_2) \qquad (14)$$

$$R^{(1)} = \frac{6\pi^2}{625} P_Q{}^2 (2J_1 + 8J_2) \qquad (15)$$

It is known that, while eq 14 works well for $\omega_0\tau_c \leq 1.5$, eq 15 is a reasonably good approximation for the longitudinal relaxation process even in the slow motion limit.

3.1.3. Slow Motion Limit. For biological macromolecules or medium-sized molecules at very high magnetic fields, it is possible that $\omega_0\tau_c \gg 1$, which is known as the slow motion limit. Because now $J_0 \gg J_1 \approx 4J_2$, $R_{II}^{(2)}$ and $R_{III}^{(2)}$ are so much larger than $R_I^{(2)}$ that their contributions to the observable spectrum are negligible. As a result, the spectrum once again exhibits a single Lorentzian line due to $R_I^{(2)}$ alone (i.e., the QCT signal) having a full width at half-height (fwhh) of

$$\Delta\nu_{1/2} = \frac{R_I^{(2)}}{\pi} = \frac{3\pi}{1000} P_Q{}^2 (16J_1 + 56J_2)$$
$$\approx (7.2 \times 10^{-3}) \left(\frac{P_Q}{\nu_0}\right)^2 \frac{1}{\tau_c} \qquad (16)$$

Note that the line width of this QCT signal is now inversely proportional to τ_c. This is exactly opposite the situations seen under the extreme narrowing condition; see eq 13. In the slow motion limit, the dynamic frequency shift (ppm) of the QCT signal is given by

$$\Delta\delta_d = \delta_{obsd} - \delta_{iso} = \frac{\Omega_I}{2\pi\nu_0} \times 10^6$$
$$\approx (-6 \times 10^3) \left(\frac{P_Q}{\nu_0}\right)^2 \qquad (17)$$

where δ_{obsd} is the observed QCT signal position (ppm) and δ_{iso} is the isotropic chemical shift (ppm). Equation 17 indicates that, in the slow motion limit, the observed QCT signal always appears at a lower frequency position from the true isotropic chemical shift position.

Here it is also important to comment on the motional window in which the above discussions are valid for the slow motion limit. Because eqs 16 and 17 are derived from Redfield's relaxation theory, they are applicable to slow molecular motions for which $(1/\omega_0)(\omega_0/\omega_Q)^2 > \tau_c \gg 1/\omega_0$, where $\omega_0 = 2\pi\nu_0$ and $\omega_Q = 2\pi C_Q$. In the context of ^{17}O QCT studies, this window for the slow motion limit corresponds approximately to 200 ns > $\tau_c \gg$ 1 ns,

assuming ν_0 = 122 MHz (21.14 T) and C_Q = 10 MHz. If the molecular motion is too slow, high-order effects are expected.[61]

3.2. Optimal Resolution in ^{17}O QCT Spectra. If the quadrupole interaction is the only relaxation mechanism, eq 16 suggests that the line width of the QCT signal should decrease monotonically as τ_c increases in the slow motion limit. However, for ^{17}O nuclei in organic and biological molecules, the shielding anisotropy (SA) interaction may contribute to the transverse relaxation process and thus the observed line width, especially at high magnetic fields. Previous studies by Lerner and Torchia[62] and by Lee and Oldfield[57] have shown the importance of SA contributions to multiexponential quadrupolar relaxation processes. It is well-known that the SA contribution to the transverse relaxation can be written as[63]

$$R_{SA}^{(2)} = \frac{2\pi^2}{45}(P_{SA}\nu_0)^2(8J_0 + 6J_1) \quad (18)$$

In eq 18, the shielding anisotropy product parameter (ppm, 10^{-6}), P_{SA}, is defined as

$$P_{SA} = \Delta\sigma\sqrt{1 + \frac{{\eta_{SA}}^2}{3}} \quad (19)$$

where $\Delta\sigma$ and η_{SA} are related to the shielding tensor components (σ_{xx}, σ_{yy}, and σ_{zz} defined according to $|\sigma_{zz} - \sigma_{iso}| \geq |\sigma_{xx} - \sigma_{iso}| \geq |\sigma_{yy} - \sigma_{iso}|$) in the following manner:

$$\Delta\sigma = \sigma_{zz} - \frac{\sigma_{xx} + \sigma_{yy}}{2} \quad (20)$$

and

$$\eta_{SA} = \frac{\sigma_{yy} - \sigma_{xx}}{\sigma_{zz} - \sigma_{iso}} \quad (21)$$

Hence, if both quadrupole and SA interactions are operative, the observed line width (and the transverse relaxation rate) in the slow motion limit becomes

$$\frac{R_{obsd}^{(2)}}{\pi} = \frac{R_I^{(2)}}{\pi} + \frac{R_{SA}^{(2)}}{\pi} \approx (7.2 \times 10^{-3})\left(\frac{P_Q}{\nu_0}\right)^2\frac{1}{\tau_c} + 1.1(P_{SA}\nu_0)^2\tau_c \quad (22)$$

It is quite interesting to note that the two terms in eq 22 exhibit an opposite dependence on the applied magnetic field. Consequently, for a given molecular system, there exists an optimal magnetic field strength at which the line width of the QCT signal is the smallest. In this regard, QCT spectroscopy for quadrupolar nuclei is analogous to the transverse relaxation optimized spectroscopy (TROSY) type experiments[64−68] now commonly used for studying spin-1/2 nuclei in biological macromolecules. It can be readily shown that the optimal condition for recording QCT spectra is

$$\nu_0^2\tau_c = \sqrt{\frac{(7.2 \times 10^{-3}){P_Q}^2}{1.1{P_{SA}}^2}} \approx (8.1 \times 10^{-2})\frac{P_Q}{P_{SA}} \quad (23)$$

and the corresponding minimal QCT line width is given by

$$(\Delta\nu_{1/2})_{min} \approx 0.18 P_Q P_{SA} \quad (24)$$

As seen from eq 23, the optimal QCT condition depends on the interplay of ν_0, τ_c, P_Q, and P_{SA}. To illustrate how the line width of ^{17}O QCT signals depends on the applied magnetic field strength, we present in Figure 4 the theoretical results for several typical oxygen-containing functional groups: carbonyl groups (P_Q = 8 MHz and P_{SA} = 500 ppm),[12,16−18,69] hydroxyl groups (P_Q = 10 MHz and P_{SA} = 50 ppm),[70−72] *C*-nitroso groups (P_Q = 16 MHz and P_{SA} = 1000 ppm),[73] and carbon monoxy or nitrosyl ligands (P_Q = 2 MHz and P_{SA} = 800 ppm).[57,74] As seen from Figure 4, within each group, although the theoretical value of $(\Delta\nu_{1/2})_{min}$ is the same, whether it is possible to achieve this optimal resolution with currently available magnetic field strength depends critically on τ_c. One general trend is that, if P_{SA} is small, it is always desirable to employ the highest magnetic field possible. On the other hand, if both P_Q and P_{SA} are large, it may become crucial to select the optimal field strength for a given molecular system to have any chance to observe ^{17}O QCT signals. Nonetheless, these results strongly suggest that ^{17}O QCT should be applicable to a wide range of biological macromolecules at moderate and high magnetic fields (e.g., >14 T).

3.3. Spectral Intensity and Nutation Behavior of QCT Signals. It is well-known in the context of solid-state NMR studies of half-integer quadrupolar nuclei that, when the RF field is much smaller than the quadrupole interaction (the so-called selective excitation condition), the relative excitation of the single-quantum coherences for a quadrupolar nucleus during the duration of an RF pulse (t_p) is given by[75,76]

$$\frac{\langle I_{x,y}^{m_I, m_I-1}\rangle}{\sum_{m_I=I}^{-I+1}\langle I_{x,y}^{m_I, m_I-1}\rangle} = \frac{3\sqrt{I(I+1) - m_I(m_I-1)}}{2I(I+1)(2I+1)}\sin(\sqrt{I(I+1) - m_I(m_I-1)}\omega_{RF}t_p) \quad (25)$$

Consequently, the QCT signal (m_I = 1/2) would exhibit a maximal excitation when

$$t_p = \frac{1}{\sqrt{I(I+1) - m_I(m_I-1)}}\frac{\pi/2}{\omega_{RF}} = \frac{1}{I + \frac{1}{2}}t_p(90^\circ) \quad (26)$$

This means that the effective 90° pulse width for the CT signal is I + 1/2 times shorter than that of a conventional 90° pulse, $t_p(90^\circ)$. In addition, eq 25 also predicts that, after an effective 90° pulse, the relative spectral intensity of the CT signal is

$$\frac{\langle I_{x,y}^{CT}\rangle}{\sum_{m_I=I}^{-I+1}\langle I_{x,y}^{m_I, m_I-1}\rangle} = \frac{3}{4I(I+1)} \quad (27)$$

For spin-5/2 nuclei such as ^{17}O, eq 27 suggests that the maximum CT signal generated by a single RF pulse is only 3/35 ≈ 8.6% of the total signal intensity under the selective excitation condition. The situation in QCT spectroscopy in the slow motion limit is analogous to the solid-state case. Thus, eqs 25−27 are also true for liquid samples in the slow motion limit, as first experimentally demonstrated by Butler and Eckert.[34] It is also interesting to point out that, if the CT signal were detected by continuous-wave (CW) NMR, the CT signal intensity would be 9/35 ≈ 25.7% of the total signal intensity, 3 times larger than that observed by the pulsed NMR method.

dx.doi.org/10.1021/ja1079207 |J. Am. Chem. Soc. 2011, 133, 920–932

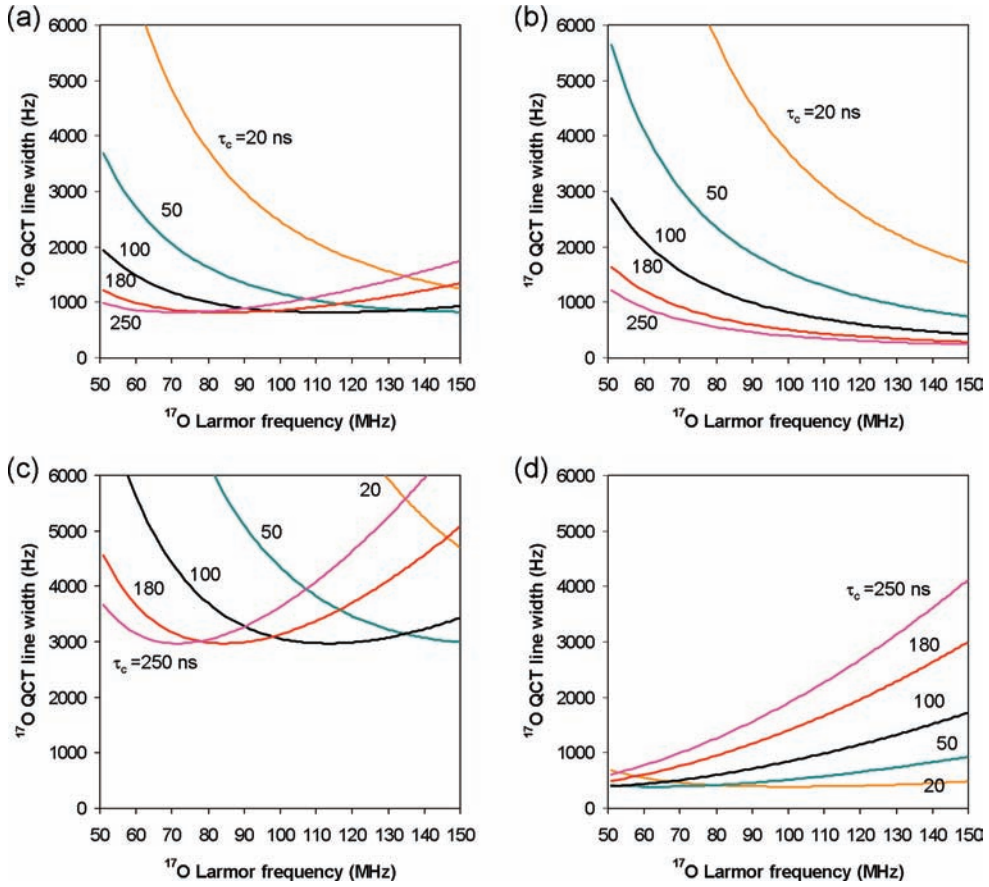

Figure 4. Theoretical results of the dependence of the ^{17}O QCT line width on τ_c, ν_0, P_Q, and P_{SA}: (a) P_Q = 8 MHz and P_{SA} = 500 ppm, (b) P_Q = 10 MHz and P_{SA} = 50 ppm, (c) P_Q = 16 MHz and P_{SA} = 1000 ppm, (d) P_Q = 2 MHz and P_{SA} = 800 ppm. As a quick reference, typical ^{17}O Larmor frequency (ν_0) values are listed here: 67.8 MHz (11.75 T), 81.4 MHz (14.1 T), 101.7 MHz (17.6 T), 108.5 MHz (18.8 T), and 122.0 MHz (21.14 T).

4. RESULTS AND DISCUSSION

Figure 5 shows the ^{17}O QCT NMR spectra of a ternary complex consisting of ovotransferrin, Al^{3+}, and [$^{17}O_4$]oxalate in aqueous solution. Ovotransferrin (OTf) belongs to a family of iron-binding proteins known as transferrins. OTf is a single-chain 80 kDa glycoprotein consisting of two homologous N- and C-lobes. Each OTf molecule is also capable of binding two Al^{3+} cations and two synergistic anions (e.g., carbonate or oxalate) with high affinity ($K_d \approx 10^{-12}$ M).[77] It can be seen from Figure 5 that, in the presence of excessive oxalate ligands, both free and protein-bound oxalates were observed in the ^{17}O NMR spectra. After ultrafiltration treatment, the very strong ^{17}O NMR signal from free oxalate ligands, $\delta(^{17}O)$ = 263 ppm, was successfully removed, leaving behind only those from protein-bound oxalate ligands. It is also important to point out that, while the resonance position (ppm) of the free ligand signal is invariant as a function of the applied magnetic field, the apparent resonance positions (ppm) of the QCT signals do change as a function of the applied field due to the presence of dynamic frequency shifts, as explained in the Theory section; see eq 17. Another way to identify QCT signals is to examine the nutation behavior as shown in Figure 6. Here the ^{17}O QCT signals from protein-bound oxalate ligands reach a maximum at ~6 μs, 3 times shorter than the 90° pulse width measured for the water signal, $t_p(90°) \approx$ 18 μs. This observation is in agreement with that predicted by eq 26. Similar nutation behaviors have been previously reported in QCT studies.[34,38]

To obtain accurate ^{17}O chemical shifts for the protein-bound ligands, we need to perform ^{17}O QCT experiments at multiple magnetic fields. Figure 7 shows the results from such QCT experiments for OTf−Al−[$^{17}O_4$]oxalate at three magnetic fields, 11.74, 14.09, and 21.14 T. Also shown in Figure 7 are the ^{17}O QCT results for a pyruvate kinase−Mg−ATP−[$^{17}O_4$]oxalate complex. PK is a tetramer consisting of four equal subunits of a total molecular mass of ca. 240 kDa. Both Mg^{2+} and K^+ are required as cofactors for optimal PK activity. In the presence of ATP, oxalate is known to bind tightly to PK.[78] In fact, a crystal structure of the PK−Mg−ATP−oxalate complex has been reported.[79] As seen clearly from Figure 7b,d, the resonance positions of the ^{17}O QCT signals change as a function of the applied magnetic field in a way predicted by eq 17. That is, the resonance position (ppm) of a QCT signal changes linearly with $(1/\nu_0)^2$. Thus, the true ^{17}O chemical shift, δ_{iso}, and the quadrupole product parameter, P_Q, can be determined from the y-intercept and the slope of each of the straight lines, respectively; see Figure 7. From such an analysis, we obtained the values of δ_{iso} and P_Q for each of the four oxygen sites of the protein-bound oxalate ligand. The results are summarized in Table 1, and the detailed experimental values are provided in the Supporting Information. We should point out that, although the homologous N- and C-lobes of OTf in the complexed form are slightly different, as seen in their ^{13}C and ^{27}Al NMR spectra,[38] we have observed only one set of ^{17}O QCT signals in OTf−Al−[$^{17}O_4$]oxalate. This is not totally unexpected because the

dx.doi.org/10.1021/ja1079207 |J. Am. Chem. Soc. 2011, 133, 920–932

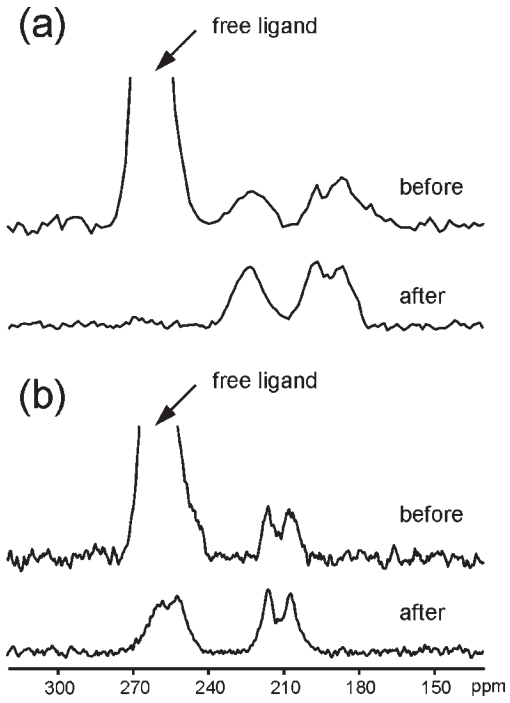

Figure 5. Experimental ^{17}O NMR spectra of OTf−Al−[$^{17}O_4$]oxalate in aqueous solution before and after ultrafiltration (3 kDa cutoff membrane) at (a) 14.09 T and (b) 21.14 T. The protein concentration was 1.5 mM. Number of transients and total experimental time (given in parentheses) for collecting each spectrum: (a) before ultrafiltration, 0.86×10^6 transients (14 h); after ultrafiltration, 2.00×10^6 transients (8 h); (b) before ultrafiltration, 0.18×10^6 transients (6 h); after ultrafiltration, 0.71×10^6 transients (3 h). Different recycle delays ranging from 5 to 100 ms were used in collecting the above spectra.

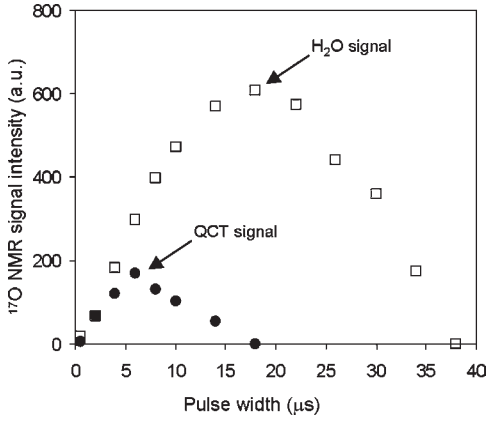

Figure 6. Dependence of the integrated ^{17}O NMR signal intensity on the excitation pulse width observed for OTf−Al−[$^{17}O_4$]oxalate (QCT signal) and for a liquid H_2O sample at 14.09 T. The RF field strength, $\omega_1/2\pi$, was 13.9 kHz.

resolution in the present ^{17}O QCT NMR spectra (fwhh ≈ 6 ppm at 21.14 T) is not sufficient to resolve sites that may differ by only 1−2 ppm. Similarly, the four subunits in the functional PK tetramer may also be slightly different. Again, we have observed only one set of ^{17}O QCT signals in PK−Mg−ATP−[$^{17}O_4$]-oxalate in aqueous solution. In light of this observation, it is perhaps not so useful to uniformly label a protein by ^{17}O (even when this may become feasible in the future). Rather, the true advantage of ^{17}O QCT is in cases where either specific amino acid residues in a protein or a ligand that is bound to a protein can be selectively labeled by ^{17}O.

As seen from Figure 7, the spectral resolution generally improves with an increase of the applied magnetic field strength. For example, at 21.14 T, four well-resolved ^{17}O NMR signals were observed for the protein-bound oxalate ligand, indicating that the four oxygen atoms within each oxalate molecule experience a quite different chemical environment (vide infra). This kind of spectral resolution for ^{17}O NMR has never been achieved before in the context of biological macromolecules. The ^{17}O QCT spectra of PK−Mg−ATP−[$^{17}O_4$]oxalate shown in Figure 7c deserve further commenting. In this particular protein sample, we deliberately kept a small amount of free [$^{17}O_4$]oxalate ligands. As seen from Figure 7c, the ^{17}O QCT signals from the protein−ligand complex at all three magnetic fields exhibit line widths comparable to (or even narrower than in some cases) those observed for the free oxalate ligand. This is quite remarkable considering the fact that the PK−Mg−ATP−[$^{17}O_4$]oxalate complex (∼240 kDa) is nearly 3000 times larger than a free oxalate ligand (88 Da). This illustrates the advantage of ^{17}O QCT spectroscopy in studying macromolecules.

Another source of information from ^{17}O QCT spectra is the observed line width as a function of the applied magnetic field. Figure 8 shows the experimental results for OTf−Al−[$^{17}O_4$]-oxalate and PK−Mg−ATP−[$^{17}O_4$]oxalate complexes at three magnetic fields. It is interesting to note that, while the line width (Hz) of the QCT signals for OTf−Al−oxalate generally decreases with an increase of the applied magnetic field, it does not decrease nearly as fast as one would expect on the basis of eq 16. Furthermore, the line width of the ^{17}O QCT signals from PK−Mg−ATP−[$^{17}O_4$]oxalate reaches a minimum at 14.09 T. These observations immediately suggest that ^{17}O SA interactions must be important in both of these systems. We were able to fit the general trends by using eq 22 with an additional constant of 100 Hz that accounts for other field-independent contributions (such as field inhomogeneity and ^{1}H−^{17}O dipolar interactions) to the observed line width. Such an analysis yielded the SA product parameter, P_{SA}, and the molecular rotational correlation time, τ_c, for both OTf−Al−oxalate and PK−Mg−ATP−oxalate. These results are also given in Table 1. For OTf−Al−oxalate, we found a τ_c value of 65 ± 10 ns at 298 K. This is in reasonably good agreement with those determined by Vogel and colleagues.[80] For PK−Mg−ATP−oxalate, the molecular tumbling is much slower, τ_c = 180 ± 10 ns, in qualitative agreement with the 10^{-7} s that is expected from the Stokes−Einstein relation for PK−Mg−ATP−oxalate (ca. 240 kDa) in aqueous solution. It is interesting to note that, while the optimal ^{17}O QCT condition for OTf−Al−oxalate (τ_c = 65 ns) is above 21.14 T, it occurs near 14.09 T for PK−Mg−ATP−oxalate (τ_c = 180 ns). Thus, the experimental observations shown in Figure 8 resemble somewhat the τ_c dependence illustrated in Figure 4a. These τ_c values also strongly suggest that the oxalate ligand is tightly bound to the protein in both complexes without any ligand exchange or local flexible motion.

As we have determined the τ_c values for OTf−Al−oxalate and PK−Mg−ATP−oxalate, we are able to characterize quantitatively the molecular motions in these systems. At 14.09 T, for example, $\omega_0\tau_c$ is equal to 33 and 92 for OTf−Al−oxalate and PK−Mg−ATP−oxalate, respectively. Indeed these systems are safely in the slow motion region. More generally, if we choose $\omega_0\tau_c \geq 10$ as a criterion for the slow motion limit, simple

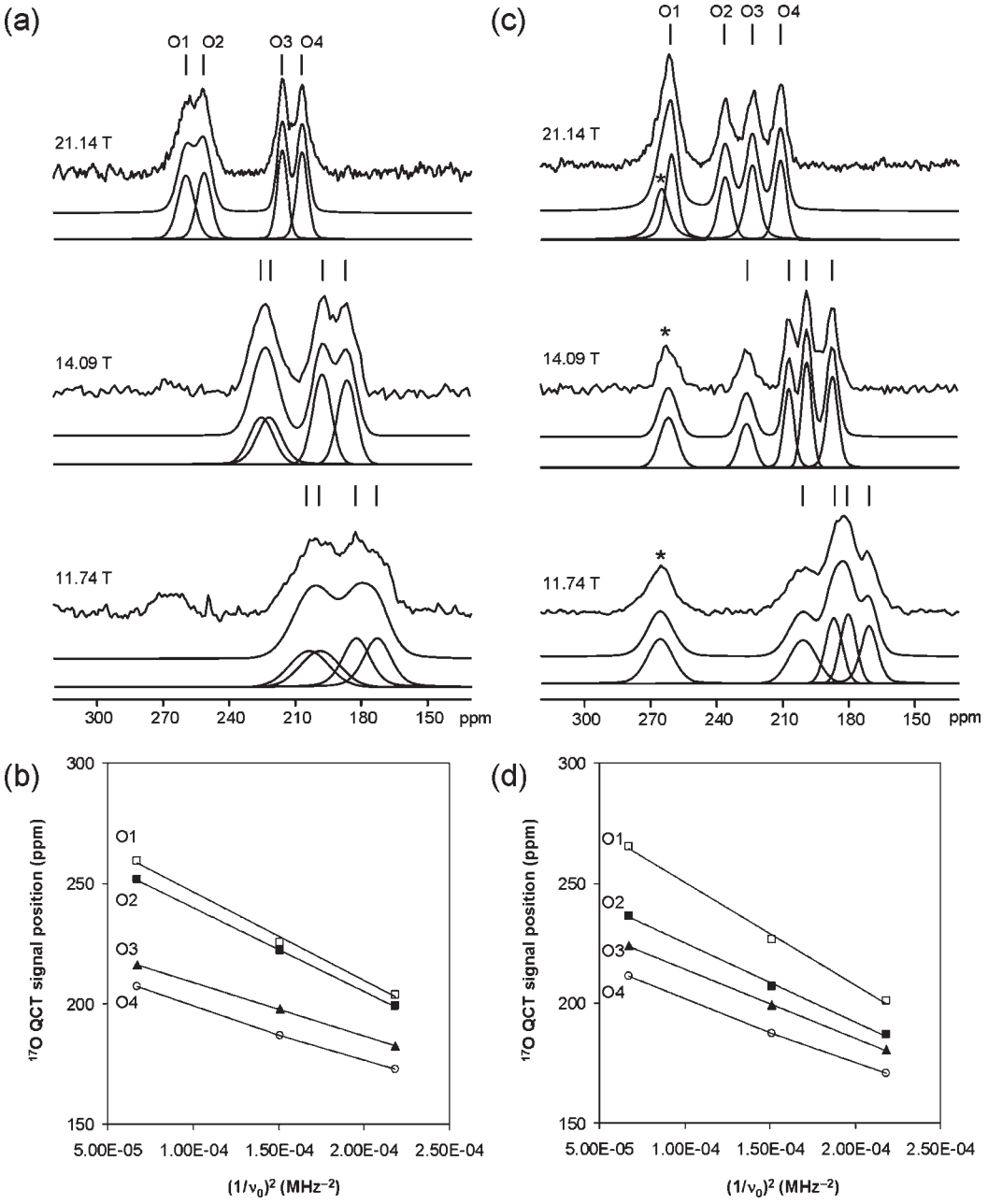

Figure 7. Experimental (upper traces) and best fitted (lower traces) ^{17}O QCT spectra and the associated data analysis for (a, b) OTf−Al−[$^{17}O_4$]-oxalate and (c, d) PK−Mg−ATP−[$^{17}O_4$]oxalate in aqueous solution. All experiments were performed at 298 K. The protein concentration was 1.5 and 0.8 mM for OTf−Al−[$^{17}O_4$]oxalate and PK−Mg−ATP−[$^{17}O_4$]oxalate, respectively. Number of transients and total experimental time (given in parentheses) for collecting each spectrum: (a) 21.14 T, 0.71 × 10^6 transients (4.9 h); 14.09 T, 2.00 × 10^6 transients (8.3 h); 11.74 T, 2.68 × 10^6 transients (11.2 h); (c) 21.14 T, 1.95 × 10^6 transients (13.5 h); 14.09 T, 3.42 × 10^6 transients (14.2 h); 11.74 T, 2.18 × 10^6 transients (9.1 h). A recycle delay of 5 ms was used in collecting all these spectra. Both the best fitted total line shapes and individual components are shown.

calculations suggest that ^{17}O QCT spectroscopy is applicable to any macromolecular system with $\tau_c \geq 20$ ns at 14.09 T. Of course, with higher magnetic fields, macromolecules suitable for ^{17}O QCT studies can be easily extended to $\tau_c < 20$ ns. This means that ^{17}O QCT spectroscopy should be applicable to a wide range of biological macromolecules with currently available moderate and ultrahigh magnetic fields.

In ^{17}O QCT spectroscopy, since the line width of QCT signals depends critically on τ_c, any factor that may change the value of τ_c for a particular system will have some impacts on the quality of QCT spectra. In the discussion that follows, we examine two of these factors: temperature and solvent viscosity. These factors were first investigated in the context of QCT studies by Andersson et al.[41] and by Butler and Eckert.[34] Figure 9 shows the ^{17}O QCT spectra obtained for an avidin−[$^{17}O_2$]biotin complex in aqueous solution at different temperatures. The signal at 275 ppm is due to the free biotin ligands in solution, whereas the signal at 220 ppm is originated from the protein-bound biotin ligands. As expected, as the temperature of the sample decreases (giving rise to a longer τ_c), the line width of the signal from free biotin ligands increases substantially. This is because free biotin ligands are under the extreme narrowing

dx.doi.org/10.1021/ja1079207 |J. Am. Chem. Soc. 2011, 133, 920–932

Table 1. Experimental ^{17}O NMR Parameters and Molecular Rotational Correlation Times Determined for Two Protein−Ligand Complexes in Aqueous Solution

system	O atom	δ_{iso}/ppm	P_Q/MHz	P_{SA}/ppm	τ_c/ns
OTf−Al−[$^{17}O_4$]oxalate	O1	283 ± 1	7.85 ± 0.05	550 ± 50	65 ± 10
	O2	275 ± 1	7.62 ± 0.05	550 ± 50	65 ± 10
	O3	231 ± 1	6.08 ± 0.05	450 ± 50	65 ± 10
	O4	222 ± 1	6.14 ± 0.05	450 ± 50	65 ± 10
PK−Mg−ATP−[$^{17}O_4$]oxalate	O1	293 ± 1	8.42 ± 0.05	450 ± 50	180 ± 10
	O2	258 ± 1	7.38 ± 0.05	410 ± 50	180 ± 10
	O3	243 ± 1	6.92 ± 0.05	410 ± 50	180 ± 10
	O4	228 ± 1	6.65 ± 0.05	410 ± 50	180 ± 10

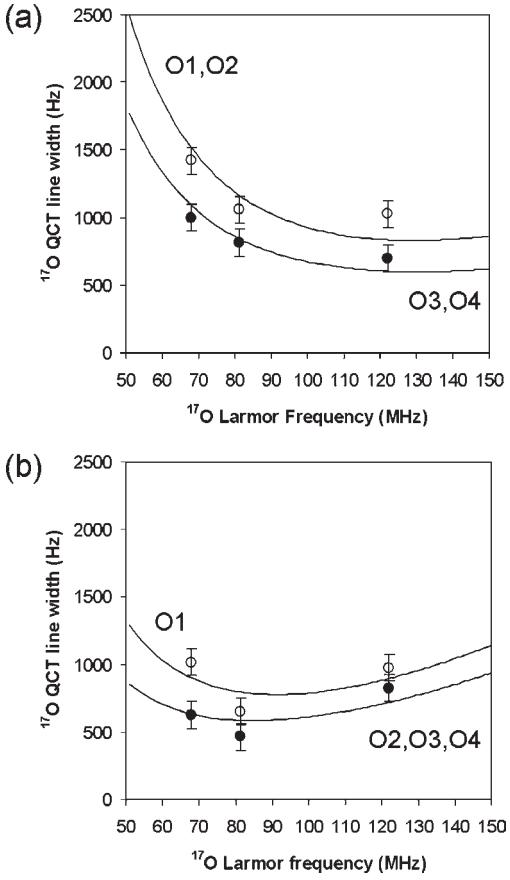

Figure 8. Experimental (data points) and calculated (lines) results of the averaged ^{17}O QCT line width as a function of the applied magnetic field for (a) OTf−Al−[$^{17}O_4$]oxalate and (b) PK−Mg−ATP−[$^{17}O_4$]-oxalate. All experiments were performed at 298 K.

condition; see eq 13. In contrast, the ^{17}O QCT signal from protein-bound biotin ligands becomes narrower with a decrease in temperature, because the protein−ligand complex is in the slow motion limit; see eq 16. As a result, the relative intensity of the QCT signal increases dramatically at low temperatures. This illustrates that it is preferable, in general, to perform QCT experiments at low temperatures. Of course, for proteins in aqueous solution, the operating temperature range is rather limited. Figure 10 shows the ^{17}O QCT spectra obtained for the same PK−Mg−ATP−[$^{17}O_4$]oxalate complex in pure aqueous solution and in 20% (v/v) glycerol/water solution. In the aqueous solution, a large signal arising from the free oxalate

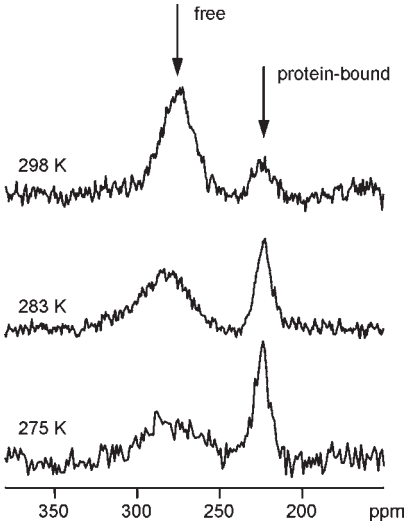

Figure 9. Experimental variable-temperature ^{17}O NMR spectra of the avidin−[$^{17}O_2$]biotin complex in aqueous solution. The protein concentration was 1 mM. All spectra were recorded at 14.09 T. For each spectrum, a total of 0.22 × 10^6 transients were recorded with a recycle time of 10 ms.

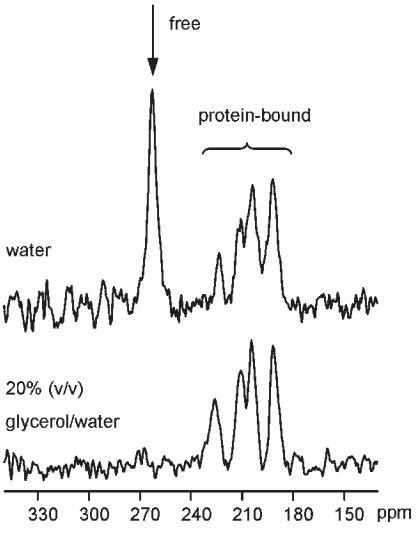

Figure 10. Experimental ^{17}O NMR spectra of PK−Mg−ATP−[$^{17}O_4$]oxalate in different solvents. All experiments were performed at 298 K. The protein concentration was 0.3 mM. Number of transients and total experimental time (given in parentheses) for collecting each spectrum: in water, 1.4 × 10^6 transients (5.8 h); in 20% (v/v) glycerol/water, 2.4 × 10^6 transients (10 h).

dx.doi.org/10.1021/ja1079207 |J. Am. Chem. Soc. 2011, 133, 920–932

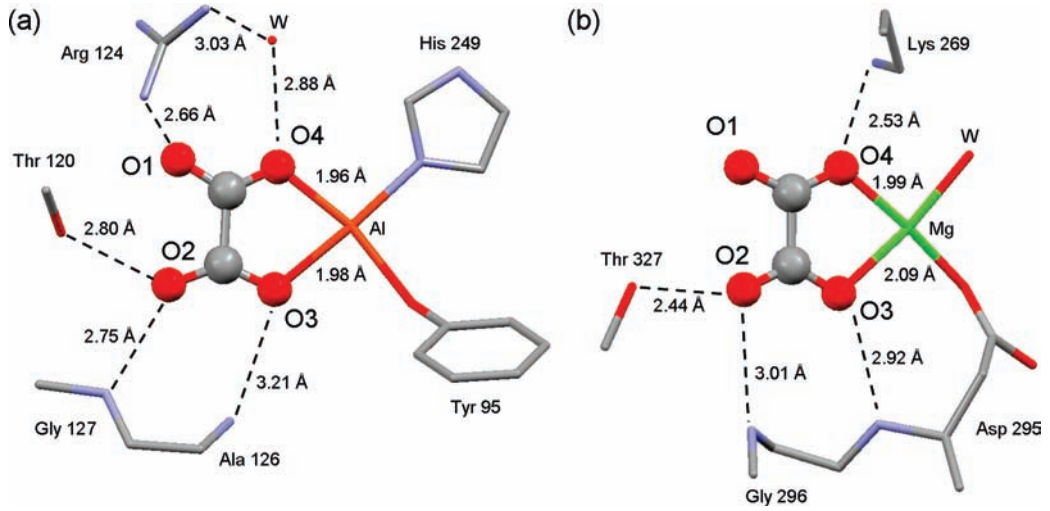

Figure 11. Partial crystal structures of (a) OTf−Al−oxalate and (b) PK−Mg−ATP−oxalate to illustrate the oxalate binding environment. For the sake of clarity, the following axial ligands are omitted: Tyr 188 and Asp 63 at the Al center in (a) and Glu 271 and γ-phosphate at the Mg center in (b). See the text for a discussion.

ligands was observed at 263 ppm, in addition to the four QCT signals from the protein-bound oxalate ligands. In the 20% (v/v) glycerol/water solution, however, the signal from free oxalate ligands is broadened beyond detection, whereas the QCT signals remain essentially unchanged. This suggests that τ_c for free oxalate ligands is increased substantially on going from aqueous to 20% glycerol/water solution, leading to significant line broadening as predicted by eq 13. For the PK−Mg−ATP−oxalate complex, however, because the dependence of the QCT line width on τ_c is rather shallow at large τ_c values, as seen in Figure 8b, the addition of 20% glycerol has only a minimal effect on the observed QCT line width. Therefore, one can utilize this large discrepancy in τ_c values to "filter out" signals from small molecules (i.e., spectral editing). These results illustrate that both temperature and solvent viscosity can be used either for achieving optimal resolution or for spectral editing. In principle, one may also use multiple-quantum filtering experiments[46,47] to eliminate signals from small molecules, but the sensitivity of that experiment may not be sufficient to be useful for studying biological macromolecules.

Now that we have demonstrated ^{17}O QCT spectroscopy and determined new ^{17}O NMR parameters for protein-bound ligands, we turn our attention to the interpretation of these new ^{17}O NMR parameters and their relationships to chemical bonding and molecular structure. The fact that a common ligand, oxalate, was used in OTf−Al−oxalate and PK−Mg−ATP−oxalate allows us to analyze results from both complexes together. Figure 11 shows the oxalate binding environment in OTf−Al−oxalate and PK−Mg−ATP−oxalate complexes. While the structure for PK−Mg−ATP−oxalate is based on a genuine crystal structure (PDB ID 1AU5),[79] the structure for OTf−Al−oxalate is constructed by first replacing the Fe^{3+} center in the crystal structure of human serum transferrin−Fe^{3+}−oxalate (PDB ID 1RYO)[81] by Al^{3+} and then performing partial geometry optimization for the oxalate ligand as described previously by us.[22] The overall structures around the oxalate binding site in these two very different proteins are remarkably similar. In both cases, the oxalate ligand is bound to a metal center in the bidentate mode. For convenience, we refer to the two oxygen atoms of the oxalate ligand that are bound to a metal center as the "coordination end" and the other two oxygen atoms as the "open end". On the basis of our previous knowledge about the relationship between ^{17}O NMR parameters and chemical bonding (i.e., metal−ligand and hydrogen-bonding interactions)[9] and the trend reported by Wong et al.[82] for some simple oxalate−metal systems, we can easily assign O_1 and O_2 to the open end and O3 and O4 to the coordination end of the oxalate ligand. As seen from Figure 11, in both complexes, one of the two oxygen atoms within the coordination end, O4, is involved in a very strong hydrogen bond, in addition to the metal−ligand interaction. In particular, while in OTf−Al−oxalate O4 is hydrogen bonded to a water molecule with an O4···O_w distance of 2.88 Å, O4 in PK−Mg−ATP−oxalate is hydrogen bonded to the NH_3^+ group from Lys 269 with an O4···N distance of 2.53 Å. These strong hydrogen-bonding interactions cause a small reduction in both δ_{iso} and P_Q for O4 as compared with those for O3. Interestingly, the two oxygen atoms within the open end of the oxalate also experience different hydrogen bonding interactions. In OTf−Al−oxalate, O1 is strongly hydrogen bonded to the side chain of Arg 124 ($r_{O\cdots N}$ = 2.66 Å), but O2 is involved in two hydrogen bonds ($r_{O\cdots O}$ = 2.80 Å and $r_{O\cdots N}$ = 2.75 Å). As a result, O2 exhibits slightly smaller δ_{iso} and P_Q than does O1. In PK−Mg−ATP−oxalate, the structural difference between O1 and O2 is even larger. In particular, while O2 is involved in two hydrogen bonds ($r_{O\cdots O}$ = 2.44 Å and $r_{O\cdots N}$ = 3.01 Å), O1 is free of any hydrogen-bonding interaction. Therefore, O1 and O2 in PK−Mg−ATP−oxalate have quite different δ_{iso} and P_Q values. It is also interesting to note the hydrogen-bonding difference between the two O2 atoms in the two complexes. Although both O2 atoms are involved in two hydrogen bonds, O2 in PK−Mg−ATP−oxalate is involved in a very strong hydrogen bond to the side chain of Thr 327 ($r_{O\cdots O}$ = 2.44 Å). This explains why O2 in PK−Mg−ATP−oxalate has δ_{iso} = 258 ppm, a value that is smaller than that of O2 in OTf−Al−oxalate by 17 ppm. In general, it is well-known that the stronger the hydrogen bonding interaction that an oxalate oxygen atom is involved in, the smaller the values of its δ_{iso} and P_Q.[9] In fact, there exists a correlation between δ_{iso} and P_Q observed for the oxalate ligands as shown in Figure 12. This type of correlation has been found before in carbonyl compounds.[83] We also note that the ^{17}O NMR parameters obtained in this study for OTf−Al−oxalate in aqueous solution are in excellent agreement with those measured from our recent solid-state ^{17}O NMR study.[22]

dx.doi.org/10.1021/ja1079207 |J. Am. Chem. Soc. 2011, 133, 920–932

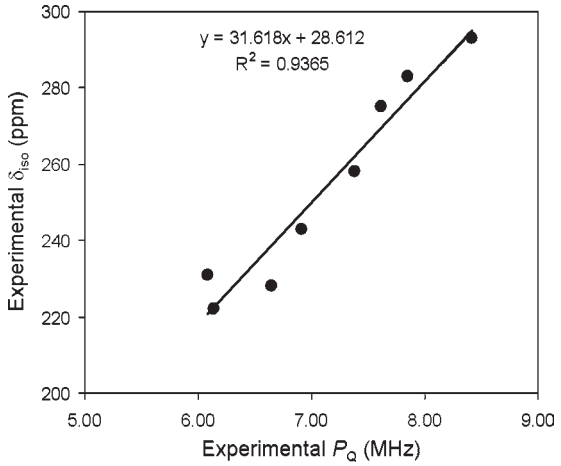

Figure 12. Correlation between experimental ^{17}O quadrupole product parameters (P_Q) and isotropic chemical shifts (δ_{iso}) observed for oxalate ligands bound to OTf and PK. The data are given in Table 1.

This suggests that OTf−Al−oxalate adopts the same structure in both solution and the solid state. The data shown in Figure 12 also illustrate the remarkable sensitivity of ^{17}O NMR parameters toward chemical bonding. Depending on the actual chemical environment, δ_{iso} and P_Q for an oxalate oxygen atom can vary by 65 ppm and 2.35 MHz, respectively. Recently, we have shown that one can use solid-state ^{17}O NMR parameters to refine the molecular structure for a protein-bound ligand.[22] Similarly, we may also use ^{17}O NMR parameters obtained from QCT spectroscopy for structural refinement.

5. CONCLUSION

In this study, we have shown that QCT spectroscopy is a general method of obtaining high-resolution ^{17}O NMR spectra for large protein−ligand complexes in aqueous solution. From the ^{17}O NMR point of view, because most proteins are in the slow motion limit at moderate or high magnetic fields (ca. >14 T), we anticipate that ^{17}O QCT NMR will become a standard technique for studying biological macromolecules in aqueous solution. Another important issue is the overall sensitivity of ^{17}O QCT NMR experiments. Here we have demonstrated that ^{17}O-labeled ligands at an approximately 30% ^{17}O enrichment level can be detected in protein−ligand complexes of 240 kDa with <1 mM protein concentrations. With a combination of higher ^{17}O enrichment (e.g., 90%), longer acquisition times (e.g., 24 h), and ultrahigh magnetic fields (e.g., 21 T), the upper limit of the molecular size suitable for ^{17}O QCT can be readily increased to 400−500 kDa. Potentially, ^{17}O QCT may also be used for probing ligand exchange processes in aqueous solution. We should also emphasize that, although protein−ligand complexes are used as examples in this study, applications of this QCT approach to other biological macromolecules can be easily envisioned. For future ^{17}O QCT studies of biological macromolecules, the main challenge lies in the development of synthetic methods that allow labeling of a particular functional group within biological macromolecules with ^{17}O. It is a truly exciting prospect if all common elements found in biological macromolecules, H, C, N, P, and O, can be equally accessible by NMR spectroscopy. We believe that this work represents an important step toward this general goal.

■ ASSOCIATED CONTENT

Supporting Information. Details about the transverse and longitudinal Redfield relaxation matrices for spin 5/2 nuclei and a table containing ^{17}O QCT peak positions and line widths measured for OTf−Al−[$^{17}O_4$]oxalate and PK−Mg−ATP−[$^{17}O_4$]oxalate at three magnetic fields. This material is available free of charge via the Internet at http://pubs.acs.org.

■ AUTHOR INFORMATION

Corresponding Author
gang.wu@chem.queensu.ca

■ ACKNOWLEDGMENT

This work was supported by the Natural Sciences and Engineering Research Council (NSERC) of Canada. Access to the 900 MHz NMR spectrometer was provided by the National Ultrahigh Field NMR Facility for Solids (Ottawa, Canada), a national research facility funded by the Canada Foundation for Innovation, the Ontario Innovation Trust, Recherche Québec, the National Research Council Canada, and Bruker BioSpin and managed by the University of Ottawa (www.nmr900.ca). NSERC is acknowledged for a Major Resources Support grant. We are grateful to Dr. Eric Ye and Dr. Victor Terskikh for technical assistance in acquiring some of the ^{17}O NMR spectra on the 900 MHz NMR spectrometer. We also thank Xin Mo for assistance in synthesizing [$^{17}O_2$]biotin and in preparing the avidin−[$^{17}O_2$]biotin sample.

■ REFERENCES

(1) Klemperer, W. G. *Angew. Chem., Int. Ed. Engl.* **1978,** *17*, 246–254.
(2) Kintzinger, J. P. . In *NMR Basic Principles and Progress*; Diehl, P., Fluck, E., Kosfeld, R., Eds.; Springer-Verlag: Berlin, 1981; Vol. 17, pp 1−64.
(3) McFarlane, W.; McFarlane, H. C. E. . In *Multinuclear NMR*; Mason, J., Ed.; Plenum: New York, 1987; pp 403−416.
(4) Boykin, D. W. *^{17}O NMR Spectroscopy in Organic Chemistry*; CRC Press: Boca Raton, FL, 1991; p 325.
(5) Gerothanassis, I. P. *Prog. Nucl. Magn. Reson. Spectrosc.* **2010,** *56*, 95–197.
(6) Gerothanassis, I. P. *Prog. Nucl. Magn. Reson. Spectrosc.* **2010,** *57*, 1–110.
(7) Wu, G. *Biochem. Cell Biol.* **1998,** *76*, 429–442.
(8) Lemaitre, V.; Smith, M. E.; Watts, A. *Solid State Nucl. Magn. Reson.* **2004,** *26*, 215–235.
(9) Wu, G. *Prog. Nucl. Magn. Reson. Spectrosc.* **2008,** *52*, 118–169.
(10) Yamauchi, K.; Kuroki, S.; Ando, I.; Ozaki, T.; Shoji, A. *Chem. Phys. Lett.* **1999,** *302*, 331–336.
(11) Wu, G.; Dong, S. *J. Am. Chem. Soc.* **2001,** *123*, 9119–9125.
(12) Wu, G.; Dong, S.; Ida, R.; Reen, N. *J. Am. Chem. Soc.* **2002,** *124*, 1768–1777.
(13) Hu, J.; Chekmenev, E. Y.; Gan, Z.; Gor'kov, P. L.; Saha, S.; Brey, W. W.; Cross, T. A. *J. Am. Chem. Soc.* **2005,** *127*, 11922–11923.
(14) Lemaitre, V.; De Planque, M. R. R.; Howes, A. P.; Smith, M. E.; Dupree, R.; Watts, A. *J. Am. Chem. Soc.* **2004,** *126*, 15320–15321.
(15) Brinkmann, A.; Kentgens, A. P. M. *J. Am. Chem. Soc.* **2006,** *128*, 14758–14759.
(16) Chekmenev, E. Y.; Waddell, K. W.; Hu, J.; Gan, Z.; Wittebort, R. J.; Cross, T. A. *J. Am. Chem. Soc.* **2006,** *128*, 9849–9855.
(17) Waddell, K. W.; Chekmenev, E. Y.; Wittebort, R. J. *J. Phys. Chem. B* **2006,** *110*, 22935–22941.
(18) Kwan, I. C. M.; Mo, X.; Wu, G. *J. Am. Chem. Soc.* **2007,** *129*, 2398–2407.

(19) Wong, A.; Beevers, A. J.; Kukol, A.; Dupree, R.; Smith, M. E. *Solid State Nucl. Magn. Reson.* **2008,** *33*, 72–75.
(20) Yamauchi, K.; Okonogi, M.; Kurosu, H.; Tansho, M.; Shimizu, H.; Gullion, T.; Asakura, T. *J. Magn. Reson.* **2008,** *190*, 327–332.
(21) Hung, I.; Uldry, A.-C.; Becker-Baldus, J.; Webber, A. L.; Wong, A.; Smith, M. E.; Joyce, S. A.; Yates, J. R.; Pickard, C. J.; Dupree, R.; Brown, S. P. *J. Am. Chem. Soc.* **2009,** *131*, 1820–1834.
(22) Zhu, J.; Ye, E.; Terskikh, V.; Wu, G. *Angew. Chem., Int. Ed.* **2010,** *49*, 8399–8402.
(23) Abragam, A. *The Principles of Nuclear Magnetism*; Oxford University Press: London, 1961.
(24) Redfield, A. G. *Adv. Magn. Reson.* **1966,** *1*, 1–32.
(25) Hubbard, P. S. *J. Chem. Phys.* **1970,** *53*, 985–987.
(26) Bull, T. E. *J. Magn. Reson.* **1972,** *8*, 344–353.
(27) Reuben, J.; Luz, Z. *J. Phys. Chem.* **1976,** *80*, 1357–1361.
(28) Bull, T. E.; Forsen, S.; Turner, D. L. *J. Chem. Phys.* **1979,** *70*, 3106–3111.
(29) Werbelow, L. G. *J. Chem. Phys.* **1979,** *70*, 5381–5383.
(30) Werbelow, L.; Pouzard, G. *J. Phys. Chem.* **1981,** *85*, 3887–3891.
(31) Westlund, P. O.; Wennerstroem, H. *J. Magn. Reson.* **1982,** *50*, 451–466.
(32) Werbelow, L. . In *Encycleopedia of Nuclear Magnetic Resonance*; Grant, D. M., Harris, R. K., Eds.; John Wiley & Sons: New York, 1996; pp 1776−1783.
(33) Werbelow, L.; London, R. E. *Concepts Magn. Reson.* **1996,** *8*, 325–338.
(34) Butler, A.; Eckert, H. *J. Am. Chem. Soc.* **1989,** *111*, 2802–2809.
(35) Germann, M. W.; Aramini, J. M.; Vogel, H. J. *J. Am. Chem. Soc.* **1994,** *116*, 6971–6972.
(36) Butler, A.; Eckert, H.; Danzitz, M. J. *J. Am. Chem. Soc.* **1987,** *109*, 1864–1865.
(37) Aramini, J. M.; Germann, M. W.; Vogel, H. J. *J. Am. Chem. Soc.* **1993,** *115*, 9750–9753.
(38) Aramini, J. M.; Vogel, H. J. *J. Am. Chem. Soc.* **1993,** *115*, 245–252.
(39) Aramini, J. M.; Germann, M. W.; Vogel, H. J. *J. Magn. Reson.* **1997,** *129*, 111–114.
(40) Aramini, J. M.; Vogel, H. J. *J. Magn. Reson., Ser. B* **1996,** *110*, 182–187.
(41) Andersson, T.; Drakenberg, T.; Forsen, S.; Thulin, E.; Swaerd, M. *J. Am. Chem. Soc.* **1982,** *104*, 576–580.
(42) Aramini, J. M.; Drakenberg, T.; Hiraoki, T.; Ke, Y.; Nitta, K.; Vogel, H. J. *Biochemistry* **1992,** *31*, 6761–6768.
(43) Aramini, J. M.; Vogel, H. J. *J. Am. Chem. Soc.* **1994,** *116*, 1988–1993.
(44) Aramini, J. M.; McIntyre, D. D.; Vogel, H. J. *J. Am. Chem. Soc.* **1994,** *116*, 11506–11511.
(45) Jaccard, G.; Wimperis, S.; Bodenhausen, G. *J. Chem. Phys.* **1986,** *85*, 6282–6293.
(46) Chung, C. W.; Wimperis, S. *Chem. Phys. Lett.* **1990,** *172*, 94–98.
(47) Chung, C. W.; Wimperis, S. *Mol. Phys.* **1992,** *76*, 47–81.
(48) Werbelow, L. *J. Magn. Reson.* **1986,** *67*, 66–72.
(49) London, R. E.; LeMaster, D. M.; Werbelow, L. *J. Am. Chem. Soc.* **1994,** *116*, 8400–8401.
(50) Grzesiek, S.; Bax, A. *J. Am. Chem. Soc.* **1994,** *116*, 10196–10201.
(51) Werbelow, L.; London, R. E. *J. Chem. Phys.* **1995,** *102*, 5181–5189.
(52) Witschas, M.; Eckert, H. *J. Phys. Chem. A* **1999,** *103*, 10764–10775.
(53) Holmes, L.; Peng, L.; Heinmaa, I.; O'Dell, L. A.; Smith, M. E.; Vannier, R.-N.; Grey, C. P. *Chem. Mater.* **2008,** *20*, 3638–3648.
(54) Kurkiewicz, T.; Thrippleton, M. J.; Wimperis, S. *Chem. Phys. Lett.* **2009,** *467*, 412–416.
(55) Gerlt, J. A.; Demou, P. C.; Mehdi, S. *J. Am. Chem. Soc.* **1982,** *104*, 2848–2856.
(56) Lee, H. C.; Cummings, K.; Hall, K.; Hager, L. P.; Oldfield, E. *J. Biol. Chem.* **1988,** *263*, 16118–16124.
(57) Lee, H. C.; Oldfield, E. *J. Am. Chem. Soc.* **1989,** *111*, 1584–1590.
(58) Zhu, J.; Kwan, I. C. M.; Wu, G. *J. Am. Chem. Soc.* **2009,** *131*, 14206–14207.
(59) Cohen, M. H.; Reif, F. . In *Solid State Physics*; Seitz, F., Turnbull, D., Eds.; Academic Press Inc.: New York, 1957; Vol. 5, pp 321−438.
(60) Halle, B.; Wennerstroem, H. *J. Magn. Reson.* **1981,** *44*, 89–100.
(61) Werbelow, L. *J. Chem. Phys.* **1996,** *104*, 3457–3462.
(62) Lerner, L.; Torchia, D. A. *J. Am. Chem. Soc.* **1986,** *108*, 4264–4268.
(63) Spiess, H. W. . In *NMR Principles and Progress*; Diehl, P., Fluck, E., Kosfeld, R., Eds.; Springer-Verlag: Berlin, 1978; Vol. 15, pp 55−214.
(64) Pervushin, K.; Riek, R.; Wider, G.; Wuthrich, K. *Proc. Natl. Acad. Sci. U.S.A.* **1997,** *94*, 12366–12371.
(65) Fernandez, C.; Wider, G. *Curr. Opin. Struct. Biol.* **2003,** *13*, 570–580.
(66) Tugarinov, V.; Hwang, P.; Ollerenshaw, J. E.; Kay, L. E. *J. Am. Chem. Soc.* **2003,** *125*, 10420–10428.
(67) Ollerenshaw, J. E.; Tugarinov, V.; Kay, L. E. *Magn. Reson. Chem.* **2003,** *41*, 843–852.
(68) Tugarinov, V.; Sprangers, R.; Kay, L. E. *J. Am. Chem. Soc.* **2004,** *126*, 4921–4925.
(69) Yamada, K.; Dong, S.; Wu, G. *J. Am. Chem. Soc.* **2000,** *122*, 11602–11609.
(70) Sefzik, T. H.; Houseknecht, J. B.; Clark, T. M.; Prasad, S.; Lowary, T. L.; Gan, Z.; Grandinetti, P. J. *Chem. Phys. Lett.* **2007,** *434*, 312–315.
(71) Zhu, J.; Geris, A. J.; Wu, G. *Phys. Chem. Chem. Phys.* **2009,** *11*, 6972–6980.
(72) Zhu, J.; Lau, J. Y. C.; Wu, G. *J. Phys. Chem. B* **2010,** *114*, 11681–11688.
(73) Wu, G.; Zhu, J.; Mo, X.; Wang, R. Y.; Terskikh, V. *J. Am. Chem. Soc.* **2010,** *132*, 5143–5155.
(74) Godbout, N.; Sanders, L. K.; Salzmann, R.; Havlin, R. H.; Wojdelski, M.; Oldfield, E. *J. Am. Chem. Soc.* **1999,** *121*, 3829–3844.
(75) Man, P. P.; Klinowski, J.; Trokiner, A.; Zanni, H.; Papon, P. *Chem. Phys. Lett.* **1988,** *151*, 143–150.
(76) Freude, D.; Haase, J. . In *NMR Basic Principles and Progress*; Diehl, P., Fluck, E., Gunther, H., Kasfeld, R., Seelig, J., Eds.; Springer-Verlag: Berlin, 1993; Vol. 29, pp 1−90.
(77) Baker, E. N. *Adv. Inorg. Chem.* **1994,** *41*, 389–463.
(78) Lodato, D. T.; Reed, G. H. *Biochemistry* **1987,** *26*, 2243–2250.
(79) Larsen, T. M.; Benning, M. M.; Rayment, I.; Reed, G. H. *Biochemistry* **1998,** *37*, 6247–6255.
(80) Aramini, J. M.; Vogel, H. J. *Biochem. Cell Biol.* **1998,** *76*, 210–222.
(81) Halbrooks, P. J.; Mason, A. B.; Adams, T. E.; Briggs, S. K.; Everse, S. J. *J. Mol. Biol.* **2004,** *339*, 217–226.
(82) Wong, A.; Thurgood, G.; Dupree, R.; Smith, M. E. *Chem. Phys.* **2007,** *337*, 144–150.
(83) Wu, G.; Mason, P.; Mo, X.; Terskikh, V. *J. Phys. Chem. A* **2008,** *112*, 1024–1032.